Journal of Computer and Mathematical Sciences, *Vol.10(2),361-374 February 2019* *ISSN 0976-5727 (Print)*
(An International Research Journal), *www.compmath-journal.org* *ISSN 2319-8133 (Online)*

Unsteady Flow of Newtonian Fluid through Porous Medium in Two Vertical Cylinders with an Inclined Magnetic field

B. Veera Sankar[1*] and B. Rama Bhupal Reddy[2]

[1*]Research Scholar,
Department of Mathematics,
Rayalaseema University, Kurnool, Andhra Pradesh-518007, INDIA.
[2]Professor and Head,
Department of Mathematics,
KSRM College of Engineering, Kadapa, Andhra Pradesh-516003, INDIA.
email: veerasankar4@gmail.com, reddybrb@gmail.com.

(Received on: February 8, 2019)

ABSTRACT

In this paper, an unsteady MHD flow of a viscous incompressible and electrically conducting Newtonian non-gray optically thin fluid through porous medium in two vertical cylinders influenced by time dependent periodic pressure gradient subjected to inclined magnetic field applied in azimuthally direction with an angle of inclination ξ and in the presence of appreciable thermal radiation and periodic wall temperature. The governing equations of motion and energy are transformed into ordinary differential equations which are solved in closed form in terms of the modified Bessel functions. The induced magnetic field is neglected, assuming the magnetic Reynolds number to be considerably small. The velocity and temperature fields and skin friction, the rate of heat transfer at the surface of the cylinders, and mass flux across a normal section of the annulus are evaluated computationally and are discussed graphically.

Keywords: annular region; heat transfer; periodic pressure gradient; periodic wall temperature; porous medium; thermal radiation.

1. INTRODUCTION

The peristaltic transport through tubes /channels have attracted considerable attention due to their wide applications in medical and engineering sciences, such as, in physiology,

roller and finger pumps, sanitary fluid transport, transport of corrosive fluids etc. A number of analytical[1-6], as well as numerical and experimental[7-11] studies of peristaltic flows of different fluids have been reported. Krishna and Gangadhar Reddy[12] discussed the unsteady MHD free convection in a boundary layer flow of an electrically conducting fluid through porous medium subject to uniform transverse magnetic field over a moving infinite vertical plate in the presence of heat source and chemical reaction. Krishna and Subba Reddy[13] have investigated the simulation on the MHD forced convective flow through stumpy permeable porous medium (oil sands, sand) using Lattice Boltzmann method. Krishna and Jyothi[14] discussed the Hall effects on MHD Rotating flow of a visco-elastic fluid through a porous medium over an infinite oscillating porous plate with heat source and chemical reaction. Reddy *et al*.[15] investigated MHD flow of viscous incompressible nano-fluid through a saturating porous medium. Recently, Krishna *et al*.[16-19] discussed the MHD flows of an incompressible and electrically conducting fluid in planar channel. Veera Krishna *et al*.[20] discussed heat and mass transfer on unsteady MHD oscillatory flow of blood through porous arteriole. The effects of radiation and Hall current on an unsteady MHD free convective flow in a vertical channel filled with a porous medium have been studied by Veera Krishna *et al*.[21].

In this study, we have studied an unsteady flow of a viscous incompressible and electrically conducting Newtonian non-gray optically thin fluid through porous medium in two infinite concentric vertical cylinders influenced by time dependent periodic pressure gradient subjected to an inclined magnetic field applied in azimuthally direction with an angle of inclination ξ and in the presence of appreciable thermal radiation and periodic wall temperature.

2. FORMULATION AND SOLUTION OF THE PROBLEM

The fundamental equations governing the motion of an incompressible, viscous, radiating and electrically conducting fluid are equation of continuity:

$$\vec{\nabla}.\vec{q} = 0 \tag{1}$$

MHD momentum equation:

$$\rho\left(\frac{\partial \vec{q}}{\partial t} + (\vec{q}.\vec{\nabla})\vec{q}\right) = -\vec{\nabla}p + \mu\nabla^2\vec{q} + \vec{J}\times\vec{B}\sin\xi + \rho\vec{g} \tag{2}$$

Energy equation:

$$\rho C_p\left(\frac{\partial T}{\partial t} + (\vec{q}.\vec{\nabla})T\right) = K_T\nabla^2 T + \varphi - \vec{\nabla}.\vec{q}_r \tag{3}$$

Ohm's law for an electrically conducting fluid:

$$\vec{J} = \sigma\ \ \vec{q}\times\vec{B} \tag{4}$$

Where, all physical variables are their usual meaning.

Consider a laminar, radiative flow of an incompressible, Newtonian, electrically conducting, non-gray and optically thin fluid within an annulus, influenced by a time dependent periodic pressure gradient and a periodic temperature applied to the walls of the annulus. The annulus is assumed to be bounded by two cylinders of radii *a* and *b*, where $a < b$. A cylindrical polar coordinate system (r, θ, z) is introduced with the axis of the coaxial cylinders as the *z*-axis. A magnetic field of intensity H_0 (constant) is applied in the azimuthal direction. The physical configuration of the problem is as shown in Fig.1.

In order to make the physical model idealized, the present investigation is restricted to the following assumptions:

1. All the fluid properties are considered constants except the influence of the variation in density in the buoyancy force term.
2. The viscous dissipation of energy is negligible.
3. The radiation heat flux (q_r) in the vertical direction is considered to be negligible in comparison to that in the normal direction.

We recall that the fluid moves parallel to the *z*-axis, suggesting us to take $\vec{q}$ as $(0, 0, V_z)$. Equation (1) in (r, θ, z) system becomes $\frac{1}{r}\frac{\partial}{\partial t}(rV_z) = 0$, which yields $V_z = V_z(r,t)$, due to symmetry of the model. Proceeding with the analysis, the momentum equation takes the form

$$\rho\frac{\partial V_z}{\partial t} = -\frac{\partial p}{\partial z} + \mu\left(\frac{\partial^2 V_z}{\partial r^2} + \frac{1}{r}\frac{\partial V_z}{\partial r}\right) - \sigma\mu_e^2 H_0^2 \sin^2\xi V_z - \rho g - \frac{\mu}{\rho k}V_z \tag{5}$$

The equation of state on the basis of classical Boussinesq approximation (Bergman *et al.*[8]) is

$$\rho_s = \rho\left[1 + \beta\,(T - T_s)\right] \tag{6}$$

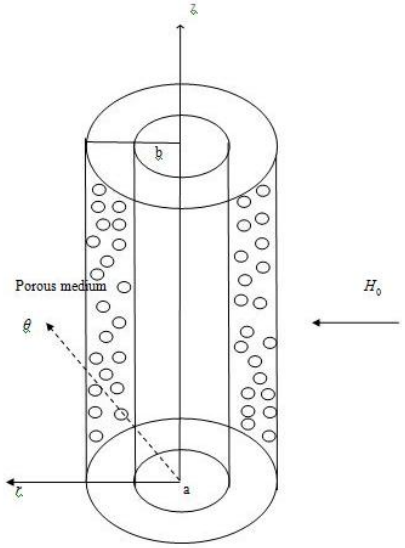

Fig. 1 Physical Configuration of the Problem

In the static condition, (5) renders $0 = -\frac{\partial p_s}{\partial z} - \rho_s g$. Utilization of this in (5) produces

$$\rho \frac{\partial V_z}{\partial t} = -\frac{\partial \ p - p_s}{\partial z} + \mu \left(\frac{\partial^2 V_z}{\partial r^2} + \frac{1}{r} \frac{\partial V_z}{\partial r} \right) - \sigma \mu_e^2 H_0^2 \sin^2 \xi V_z - \frac{\mu}{\rho k} V_z - g \ \ \rho - \rho_s \tag{7}$$

With $P = p - p_s$, the application of (6) leads to the following equation of motion:

$$\frac{\partial V_z}{\partial t} = -\frac{1}{\rho} \frac{\partial P}{\partial z} + \frac{\mu}{\rho} \left(\frac{\partial^2 V_z}{\partial r^2} + \frac{1}{r} \frac{\partial V_z}{\partial r} \right) - \frac{\sigma \mu_e^2 H_0^2 \sin^2 \xi}{\rho} V_z - \frac{\nu}{k} V_z + g\beta \ \ T - T_s \tag{8}$$

In lieu of the assumptions (2) and (3), the energy equation takes the form

$$\rho C_p \frac{\partial T}{\partial t} = K_T \left(\frac{\partial^2 T}{\partial r^2} + \frac{1}{r} \frac{\partial T}{\partial r} \right) - 4I \ \ T - T_s \tag{9}$$

On account of the axial symmetry and the annulus being infinite in the *z*-direction, the Temperature field is independent of θ and *z*. In (9), the rate of radiative heat flux in the Optically thin limit for a non-gray gas near equilibrium is due to the following formula attributed to Cogley *et al.* [9]:

$$\frac{\partial q_r}{\partial r} = 4I \ \ T - T_s \tag{10}$$

Where $I = \int_0^\infty K_{\lambda^*} \ _w \left(\frac{\partial e_{\lambda^* h}}{\partial T} \right)_w d\lambda^*$

The boundary conditions to be satisfied by (8) and (9) are

$$\left.\begin{aligned} &V_z = 0 \quad \text{at} \quad r = a; V_z = 0 \quad \text{at} \quad r = b \\ &T = T_s + T_s n_1 e^{i\alpha_1 t} \quad \text{at} \quad r = a \\ &T = T_s + T_s n_2 e^{i\alpha_1 t} \quad \text{at} \quad r = b \end{aligned}\right\} \tag{11}$$

The following non-dimensional quantities are introduced in order to normalize the model:

$$\left.\begin{aligned} &V_z^* = \frac{V_z a}{\nu}, r^* = \frac{r}{a}, z^* = \frac{z}{a}, P^* = \frac{Pa^2}{\mu\nu}, t^* = \frac{t\nu}{a^2}, \lambda = \frac{b}{a}, \psi^* = \frac{T - T_s}{T_s} \\ &M = \mu_e H_0 a \sqrt{\frac{\sigma}{\mu}}, \ K = \frac{k}{a^2}, \ \text{Gr} = \frac{g\beta a^3}{\nu^2} T_s, \ \text{Pr} = \frac{\mu C_p}{K_T}, \ Q = \frac{4la^2}{\mu C_p} \end{aligned}\right\} \tag{12}$$

The governing dimensionless forms of equations (8), (9) and the boundary conditions (11) are (Dropping asterisks):

$$\frac{\partial V_z}{\partial t} = -\frac{\partial P}{\partial z} + \left(\frac{\partial^2 V_z}{\partial r^2} + \frac{1}{r}\frac{\partial V_z}{\partial r} \right) - \left(M^2 \sin^2 \xi + \frac{1}{K} \right) - \mathrm{Gr}\psi \tag{13}$$

$$\mathrm{Pr}\frac{\partial \psi}{\partial t} = \frac{\partial^2 \psi}{\partial r^2} + \frac{1}{r}\frac{\partial \psi}{\partial r} - Q\,\mathrm{Pr}\,\psi \tag{14}$$

$$\left.\begin{array}{l} V_z = 0 \quad \text{at} \quad r = 1;\ V_z = 0 \quad \text{at} \quad r = \lambda \\ \psi = n_1 e^{i\alpha t} \quad \text{at} \quad r = 1 \\ \psi = n_2 e^{i\alpha_1 t} \quad \text{at} \quad r = \lambda \end{array}\right\} \tag{15}$$

We consider the temperature as $\psi\ r,t\ = f\ r\ e^{i\alpha t}$ with this form of ψ the equation (14) reduces to the ordinary differential equation $r^2 \dfrac{d^2 f\ r}{dr^2} + r\dfrac{df\ r}{dr} - \eta^2 r^2 f\ r\ = 0$

Where, $\eta^2 = \mathrm{Pr}(i\alpha + Q)$.

The substitution $z = ir\eta,\ f\left(\dfrac{z}{i\eta}\right) = f_1\ z$, leads us to Bessel's differential equation of order zero.

$$z^2 \frac{d^2 f_1\ z}{d^2 z^2} + z\frac{df_1\ z}{dz^2} + z^2 f_1\ z\ = 0 \tag{16}$$

The general solution to (16) is $f\ r\ = A_1 J_0\ ir\eta\ + B_1 Y_0\ ir\eta\ ,$ in which J_0 and Y_0 are Bessel's of order zero of the first kind and of the second kind, respectively, and A_1 and B_1 are constants to be determined subject to (15).

Utilizing the established identities $J_0\ ix\ = I_0\ x\ $ and $Y_0\ ix\ = -\dfrac{2}{\pi}K_0\ x\ - \dfrac{1}{i}I_0\ x\ $

and the boundary conditions (15), we are able to arrive at

$$\psi\ r,t\ = \left[A_1 I_0\ r\eta\ + B_1 \left\{ -\frac{2}{\pi}K_0\ r\eta\ - \frac{1}{i}I_0\ r\eta\ \right\} \right] \times e^{i\alpha t} \tag{17}$$

We now employ the complex variable technique solve the boundary value problem in closed form. Assuming that the pressure gradient is a periodic of *t*, we formulate

$$-\frac{\partial P}{\partial z} = P_0 e^{i\alpha t}, \tag{18}$$

Where α is the frequency parameter and P_0 is a constant which equals the pressure gradient at time $t = 0$.

Due to the assumptions made previously we consider the velocity to be interpreted as $V_z\ r,t\ = g\ r\ e^{i\alpha t}$. All these considerations in (13) finally present us with the following expression for the velocity field:

$$V_z\ r,t\ = \left(\frac{P_0}{\delta^2} + A_2 I_0\ r\delta\ + B_2 \left\{ -\frac{2}{\pi} K_0\ r\delta\ - \frac{1}{i} I_0\ r\delta\ \right\} + \right.$$

$$\left. \frac{1}{\delta^2 - \eta^2} \times \left\{ \left(\mathrm{Gr}A_1 + \mathrm{Gr}B_1 \frac{1}{i} \right) I_0\ r\eta\ + \frac{2\mathrm{Gr}B_1}{\pi} K_0\ r\eta\ \right\} \right) e^{i\alpha t} \tag{19}$$

Where,

$$\delta^2 = M^2 \sin^2 \xi + \frac{1}{K} + i\alpha$$

The viscous drags per unit area on the surface of the inner cylinder and outer cylinder, respectively, are specified by Newton's law of viscosity as mentioned below:

$$\tau_1 = -\mu \left. \frac{\partial V_z}{\partial r} \right|_{r=a} \text{ and } \tau_2 = -\mu \left. \frac{\partial V_z}{\partial r} \right|_{r=b} \tag{20}$$

The non dimensional forms of (20) are

$$\tau_1 = -\frac{\mu\nu}{a^2} \left. \frac{\partial V_z^*}{\partial r^*} \right|_{r^*=1} \quad \text{and} \quad \tau_2 = -\frac{\mu\nu}{a^2} \left. \frac{\partial V_z^*}{\partial r^*} \right|_{r^*=\lambda} \tag{21}$$

The heat fluxes q^* from the surface of the inner and outer cylinders into the fluid region are given by the Fourier law of conduction as stated below:

$$q_1^* = -K_T \left. \frac{\partial T}{\partial r} \right|_{r=a} \tag{24}$$

$$q_2^* = -K_T \left. \frac{\partial T}{\partial r} \right|_{r=b} \tag{25}$$

Using non-dimensional quantities defined, as in (12), we deduce

$$q_1^* = -\frac{K_T T_s}{a} \left. \frac{\partial \psi^*}{\partial r^*} \right|_{r^*=1} \quad \text{and} \quad q_1^* = -\frac{K_T T_s}{a} \left. \frac{\partial \psi^*}{\partial r^*} \right|_{r^*=\lambda} \tag{26}$$

The coefficients of heat transfer (Nusselt number) on the surface of the inner and outer cylinder are, respectively,

$$Nu_1 = \frac{q_1^* a}{K_T T_s} = -\left. \frac{\partial \psi}{\partial r} \right|_{r=1} = -\left[A_1 \eta I_{-1}\ \eta\ - B_1 \eta \left\{ \frac{2}{\pi} K_{-1}\ \eta\ - \frac{1}{i} I_{-1}\ \eta\ \right\} \right] e^{i\alpha t} \tag{27}$$

$$Nu_2 = \frac{q_2^* a}{K_T T_s} = -\left. \frac{\partial \psi}{\partial r} \right|_{r=\lambda} = -\left[A_1 \eta I_{-1}\ \lambda\eta\ - B_1 \eta \left\{ \frac{2}{\pi} K_{-1}\ \lambda\eta\ - \frac{1}{i} I_{-1}\ \lambda\eta\ \right\} \right] e^{i\alpha t} \tag{28}$$

The total discharge of flux (mass flux) per unit time is give

$$M_f = \int_0^{2\pi}\int_1^{\lambda} V_z r dr d\theta \tag{29}$$

3. RESULTS AND DISCUSSION

The Flow governed by the non-dimensional parameters on the velocity field, temperature field, the mass flux, the coefficient of skin friction, and the Nusselt number by assigning some arbitrarily chosen specific values to the physical parameters. The results are presented in Figures 2 to 10 and Tables 1-4. In most of the cases of our investigation, the value of the Prandtl number Pr is chosen to be 0.025 which corresponds to mercury at 20°C and at 1 atmospheric pressure. In Table 1, Pr is specified to be 0.71 and $\xi = \pi/6$, which represents air at 20°C and at 1 atmospheric pressure. Figures 2 to 7 demonstrate the velocity profiles under the influence of *M*, *K*, *Q*, Gr , Pr and α respectively.

The Hartmann number *M* is united with the ratio of the magnetic body force (Lorentz force) to viscous force. It is evident from the Fig. 2 that, an increase in the values of the Hartmann number *M* causes retardation to the fluid flow indicating the fact that the imposition of the azimuthal magnetic field decelerates the flow and consequently the thickness of the velocity boundary layer gets diminished. This observation is consistent with the physical fact that the Lorentz force that appears due to the interaction of the magnetic field and the fluid velocity resists the corresponding fluid flow, resulting in the velocity to decrease gradually. The velocity enhances with increasing the permeability of the porous medium throughout the fluid region (Fig. 3). We also concluded that, lower the permeability lesser the fluid speed is observed in the cylinder. The radiation parameter *Q* registers the effect of thermal radiation. Retardation in fluid flow under the effect of thermal radiation is also observed and this is visualized in Fig.4. Thermal radiation results in a fall in thermal energy and the physics of this situation indicate a loss in kinetic energy of the fluid; as a consequence the fluid velocity is inhibited substantially. The Grashof number is the ratio of the buoyancy force to viscous force. Fig.5 depicts that buoyancy force causes the fluid flow to accelerate and this is in good agreement to the observations of known theory. We may conclude that the behaviour of the velocity profile is fairly consistent with the known laws of physics. Pr (Prandtl number) is the ratio of the momentum diffusivity (kinematic viscosity) to thermal diffusivity. Fig.6 shows how the velocity field is affected corresponding to an increase in the values of Pr. We evident that an increase in Pr means a fall in thermal diffusivity for the model under consideration. It is learnt from this figure that when the thermal diffusivity of the fluid is reduced, the flow gets decelerated substantially which may be linked to the fact that a low thermal diffusivity leads to a corresponding decrease in the kinetic energy of the molecules of the fluid, which in turn affects the fluid velocity unpleasantly. We noticed from the Fig. 7 that the magnitude of the velocity reduces with increasing frequency parameter α throughout the fluid region.

Figs.8 to10 delineate the influence of α, Pr, and Q on the temperature profile of the fluid. An interesting observation is made from Fig.8 which suggests that the fluid temperature can be diminished comprehensively by raising the frequency parameter. This presents us with an innovative mechanism for controlling and regularizing the fluid temperature on enhancement of the frequency parameter. It is inferred from Fig. 9 that the reduction in fluid temperature is directly proportional to the diminution in thermal diffusivity. Further, Figure 10 registers the fact that the fluid temperature gets lowered with an increasing dissipation of thermal energy caused due to thermal radiation.

The variations in skin friction with respect to the frequency parameter α under the influence of M, K, Q and Gr in both the inner and the outer walls of the annulus are presented in Table 1. The magnitude of the skin friction reduces with increasing the intensity of the magnetic field being the other parameters fixed. This has been observed in the entire inner and outer walls of the cylinder. The magnitude of the skin friction enhances initially and then gradually decreases inner walls of the cylinder with increasing permeability. The similar behaviour is observed at the outer wall of the cylinder. We note that the effect of thermal radiation parameter is highly unpronounced on the friction at both walls of the annulus. The magnitude of the skin friction is boost up with increasing Grashof number Gr at both wall of the cylinder. The skin friction reduces with increasing frequency parameter α and angle of inclination ξ in both cylinders.

Table 2 illustrate how the rate of heat transfer from the walls to the fluid is influenced by Pr and α with an increase in radiation parameter Q. It is observed that as thermal diffusivity of the fluid gets reduced, increased rate of heat transfer from one of the walls is evident, provided that the thermal radiation is assumed to be constant. An enhancement of the frequency parameter leads to a comprehensive grows thin the rate of heat transfer at the walls. This property is, in fact, dependent on the Prandtl number of the fluid. When air is used a completely different behaviour is marked for Nusselt number at the walls of the annulus. This motivates us to comment that the fluid must be carefully selected if different rates of heat transfer are desired at the inner and the outer walls of the annulus.

The effects of M, K, Q, Gr, Pr and α on the mass flux are presented in Table 3. This demonstrate that the mass flux changes its direction periodically which may be accredited to the pressure gradient being periodic in nature. An increase in Gr or K results in the mass flux to increase in the direction of the fluid flow and this may be attributed to the buoyancy forces acting on the fluid and also it causes the permeability. However, A reverse trend in mass flux direction with an increase in M, Q as well as Pr. The observations are consistent with those made in the case of Figs. 2,4 and 6, respectively. All three figures lead us to conclude that the parameters M, K, Gr, Pr, and Q have significant contributions in regulating the amount of total discharge of fluid through the annulus and they may be adjusted conveniently to control the mass flux. It is evident that when the frequency parameter α or an angle of inclination ξ increases the wave length of the mass flux profile reduces in magnitude throughout the fluid region.

Table 4 Represent the comparison of the results when the parameter $K \to \infty$. We observe that, it is an excellent agreement with the results of Ahmed *et al*.[22].

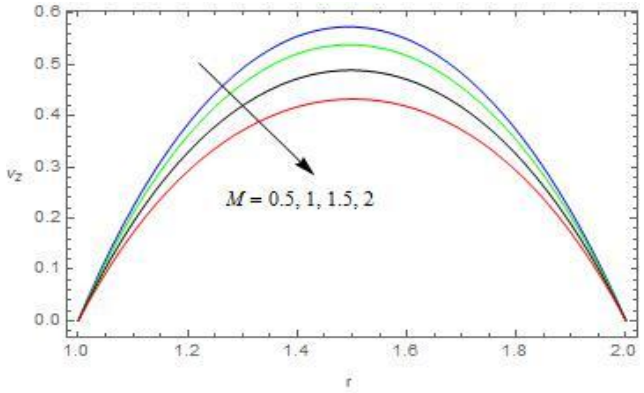

Fig.2 The velocity against M with $K = 0.5, \mathrm{Gr} = 3, \mathrm{Pr} = 0.71, Q = 2, \alpha = 0.01$

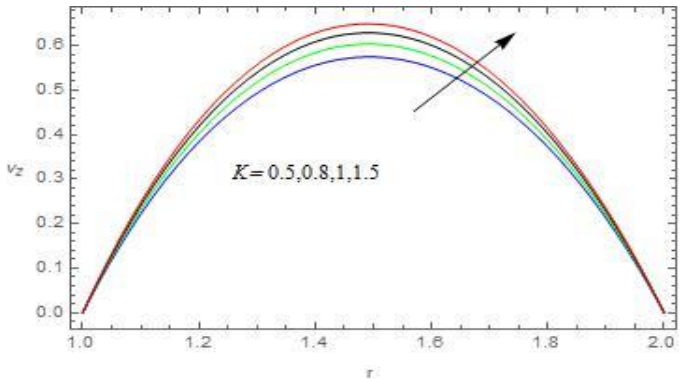

Fig.3 The velocity against K with $M = 0.5, \mathrm{Gr} = 3, \mathrm{Pr} = 0.71, Q = 2, \alpha = 0.01$

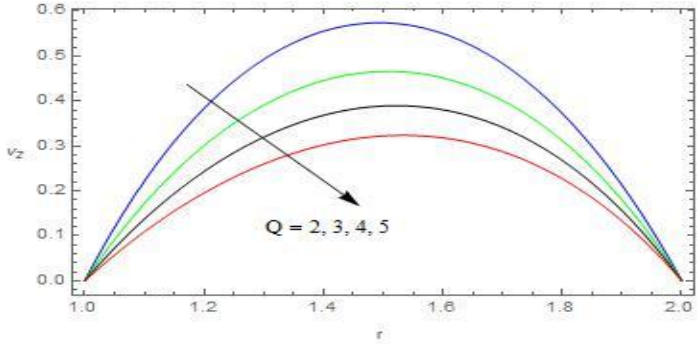

Fig.4 The velocity against Q with $M = 0.5, \mathrm{Gr} = 3, \mathrm{Pr} = 0.71, K = 0.5, \alpha = 0.01$

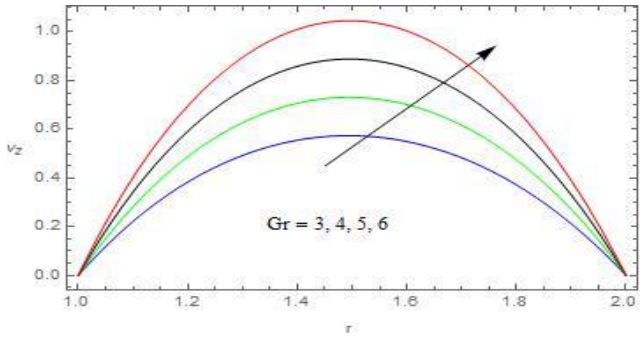

Fig.5 The velocity against Gr with $M = 0.5, K = 0.5, \Pr = 0.71, Q = 2, \alpha = 0.01$

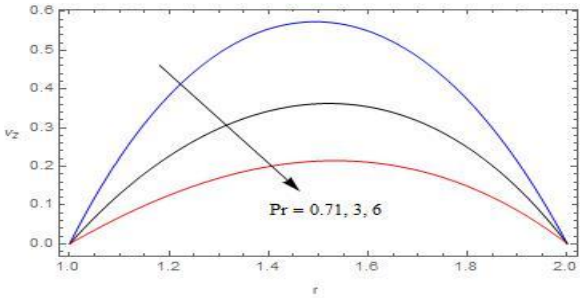

Fig.6 The velocity against Pr with $M = 0.5, K = 0.5, \mathrm{Gr} = 3, Q = 2, \alpha = 0.01$

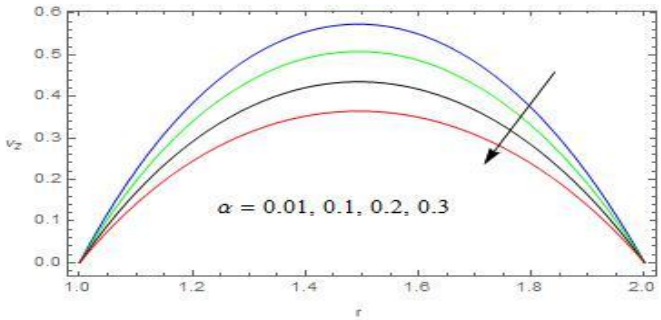

Fig.7 The velocity against α with $M = 0.5, K = 0.5, \mathrm{Gr} = 3, Q = 2, \Pr = 0.71$

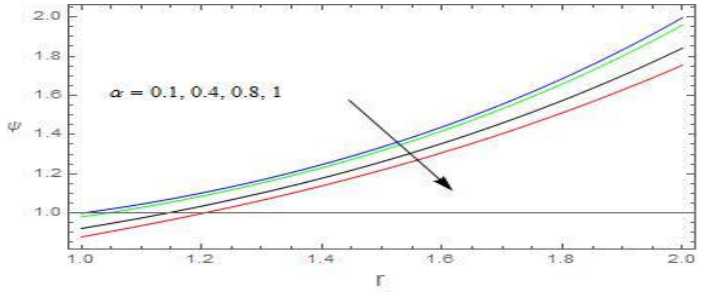

Fig.8 The Temperature Profile against α with $\Pr = 0.71$, $Q = 2$,

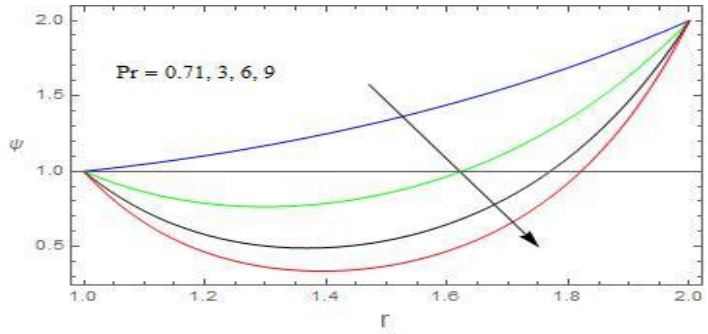

Fig.9 The Temperature Profile against Pr with $\alpha = 0.1, Q = 2,$

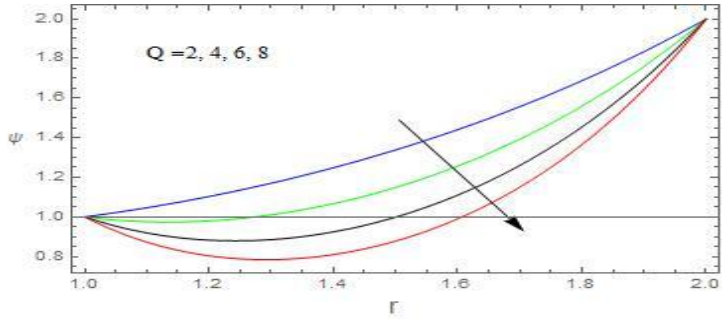

Fig.10 The Temperature Profile against Q with $\Pr = 0.71, \alpha = 0.1,$

Table 1. Skin friction

M	K	Q	Gr	α	ξ	Inner wall	Outer walls
0.5	0.5	2	3	0.5	$\pi/6$	5.65899	5.85569
1						5.45787	5.74855
1.5						5.25447	5.65589
	0.8					6.25221	6.85548
	1					5.87745	6.45221
		4				4.52662	4.85478
		6				2.36525	2.85547
			4			6.25545	6.96658
			5			8.52466	9.66522
				0.8		4.52663	5.21458
				1		2.15887	4.52265
					$\pi/4$	5.55266	5.63625
					$\pi/3$	5.41152	5.48557

Table. 2 Nusselt number

Pr	α	Q	Nu_1	Nu_2
0.025(Mercury)	0.01	5	1.31022	0.755768
0.050			1.2259	0.882613
0.075			1.14453	1.01203
	0.4		1.2346	0.630674
	0.6		1.17866	0.556051
		8	1.25839	0.829718
		10	1.22612	0.883162
0.71 (Air)	0.01	5	-19.2219	-99.3967
	0.4		1.2346	0.630674
	0.6		1.17866	0.556051
		8	1.25839	0.829718
		10	1.22612	0.883162

Table 3. Mass flux

M	K	Q	Gr	Pr	α	ξ	M_f
0.5	0.5	2	3	0.71	0.5	$\pi/6$	8.524464
1							6.521454
1.5							3.220155
	0.8						10.25665
	1						12.02214
		4					7.145822
		6					6.014558
			4				11.25548
			5				13.25688
				6			6.332569
				9			5.001452
					0.8		7.998596
					1		7.255484
						$\pi/4$	6.254885
						$\pi/3$	4.211458

Table. 4 Comparison of Results ($n_1 = 1, n_2 = 2, t = 0.5, \lambda = 2, \alpha = 0.01, P_0 = 1$)

M	Q	Gr	Previous Results N. Ahmed et al. [22]	Present Results $K \to \infty$
0.5	2	3	0.692777	0.692776
1			0.643053	0.643052
1.5			0.574032	0.574031
	4		0.470203	0.470204
	6		0.311263	0.311262
		4	0.882709	0.882708
		5	1.07264	0.07265

4. CONCLUSIONS

1. An increase in the Hartmann number M or an angle of inclination causes the fluid flow to be retarded.
2. The flow gets decelerated and therefore mass flux gets reduced corresponding to a reduction in the thermal diffusivity of the fluid.
3. Retardation in the fluid flow and a decrease in mass flux are observed with an increase in thermal radiation.
4. The buoyancy force causes the fluid flow to accelerate, thereby causing the mass flux to increase proportionately.
5. A reduction in fluid temperature is directly proportional to the diminution in thermal diffusivity.
6. Fluid temperature can be reduced by increasing the frequency parameter associated with the fluid flow.
7. Viscous drags at the inner and outer walls have identical magnitude but they act in opposite directions.
8. Friction at the walls increases with an increase in thermal Grashof number, but it diminishes with an increase in Prandtl number and radiation parameter, respectively.
9. The rate of heat transfer at either walls of the annulus with increasing frequency parameter depends on the Prandtl number of the fluid.

REFERENCES

1. Burns J C, Parkes T. Peristaltic motion. *J Fluid Mech*.; 29:731-743 (1967).
2. Fung Y C, Yih C S. Peristaltic transport, *Trans. ASME J Appl Mech*.; 35: 669-675 (1968).
3. Jaffrin M Y. Inertia and streamline curvature effects on peristaltic pumping. *Int J Engng Sci*.; 11: 681-699 (1973).
4. Ramachandra Rao A, Usha S. Peristaltic transport of two immiscible viscous fluid in a circular tube. *J Fluid Mech*.; 298: 271-285 (1995).
5. Shapiro A H, Jaffrin MY, Weinberg S L. Peristaltic pumping with long wavelengths at low Reynolds number. *J Fluid Mech*.; 37:799-825 (1969).
6. Siddiqui AM, Schwarz WH. Peristaltic flow of a second order fluid in tubes, *J. Non-Newtonian Fluid Mech*.; 53:257- 284 (1994).
7. Latham TW. Fluid motions in peristaltic pump, MS Thesis, MIT, Cambridge, *Massachusetts*, (1966).
8. Weinberg SL, Eckistein EC, Shapiro AH. An experimental study of peristaltic pumping. *J Fluid Mech*.; 49: 461- 497 (1971).
9. Takabatake S, Ayukawa K. Numerical study of twodimensional peristaltic flow. *J Fluid Mech*.; 122: 439- 465 (1982).
10. Takabatake S, Ayukawa K, Mori A. Peristaltic pumping in circular tubes: A numerical study of fluid transport and its efficiency. *J Fluid Mech*.;193: 267-283 (1988).
11. Tang D, Rankin S. Numerical and asymptotic solutions for peristaltic motion of nonlinear viscous flows with elastic free boundaries. *Siam J Sci Comput*.; 14 :1300-1319 (1993).

12. M.Veera Krishna, M.Gangadhar Reddy, MHD Free Convective Boundary Layer Flow through Porous medium Past a Moving Vertical Plate with Heat Source and Chemical Reaction, *Materials Today: Proceedings*, vol. 5, pp. 91–98, (2018). https://doi.org/10.1016/j.matpr.2017.11.058.
13. M.Veera Krishna, G.Subba Reddy, MHD Forced Convective flow of Non-Newtonian fluid through Stumpy Permeable Porous medium, *Materials Today: Proceedings*, vol. 5, pp. 175–183, (2018). https://doi.org/10.1016/j.matpr.2017.11.069.
14. M.Veera Krishna, Kamboji Jyotghi, Hall effects on MHD Rotating flow of a Visco-elastic Fluid through a Porous medium Over an Infinite Oscillating Porous Plate with Heat source and Chemical reaction, *Materials Today: Proceedings*, vol. 5, pp. 367–380, (2018). https://doi.org/10.1016/j.matpr.2017.11.094.
15. B. Siva Kumar Reddy, M. Veera Krishna , K.V.S.N. Rao, R. Bhuvana Vijaya, HAM Solutions on MHD flow of nano-fluid through saturated porous medium with Hall effects, *Materials Today: Proceedings*, vol. 5, pp. 120–131, (2018). https://doi.org/10.1016/j.matpr.2017.11.062.
16. Veera Krishna.M and B.V.Swarnalathamma, Convective Heat and Mass Transfer on MHD Peristaltic Flow of Williamson Fluid with the Effect of Inclined Magnetic Field," *AIP Conference Proceedings*, vol. 1728, p. 020461, (2016). DOI: 10.1063/1.4946512
17. Swarnalathamma. B. V. and M. Veera Krishna, Peristaltic hemodynamic flow of couple stress fluid through a porous medium under the influence of magnetic field with slip effect *AIP Conference Proceedings*, vol. 1728, p. 020603, (2016). DOI: 10.1063/1.4946654.
18. Veera Krishna.M and M.Gangadhar Reddy MHD free convective rotating flow of Visco-elastic fluid past an infinite vertical oscillating porous plate with chemical reaction, IOP Conf. Series: Materials Science and Engineering, vol. 149, p. 012217, (2016). DOI: 10.1088/1757-899X/149/1/012217.
19. Veera Krishna.M and G.Subba Reddy Unsteady MHD convective flow of Second grade fluid through a porous medium in a Rotating parallel plate channel with temperature dependent source, *IOP Conf. Series: Materials Science and Engineering*, vol. 149, p. 012216, (2016). DOI**:** 10.1088/1757-899X/149/1/012216.
20. Veera Krishna.M., B.V.Swarnalathamma and J. Prakash, "Heat and mass transfer on unsteady MHD Oscillatory flow of blood through porous arteriole, Applications of Fluid Dynamics, *Lecture Notes in Mechanical Engineering*, vol. XXII, pp. 207-224, (2018). Doi: 10.1007/978-981-10-5329-0_14.
21. M.Veera Krishna, G.Subba Reddy, A.J.Chamkha, "Hall effects on unsteady MHD oscillatory free convective flow of second grade fluid through porous medium between two vertical plates," *Physics of Fluids*, vol. 30, 023106 (2018); doi: 10.1063/1.5010863
22. Nazibuddin Ahmed, Manas Dutta, Heat transfer in an unsteady MHD flow through an infinite annulus with radiation, Boundary value problems, 11, pp. 2-17 (2015). DOI :10.1186/s13661-014-0279-z